

EFFECT OF TEMPERATURE AND STRAIN RATE ON HARDENING OF METALLIC MATERIALS

Novotný R.¹, Šebek F.²

Abstract: *The influence of temperature and strain rate on the hardening behaviour of three metallic materials is studied. Standard tensile tests were carried out under quasi-static, dynamic, and elevated temperature conditions, including static tensile tests with loading pauses to determine the static stress–strain response of AISI 316L steel, Inconel 718 and EN AW 2024-T351. Then the constitutive model was calibrated using a particle swarm optimization and subsequently validated through finite element simulations performed in LS-DYNA. The calibrated models showed good agreement with the experimental data up to the ultimate tensile strength. Larger errors occurred beyond the ultimate tensile strength due to a slight overestimation of the strain hardening exponent. The thermal softening parameter was not identified for Inconel 718 because elevated-temperature tests were not performed for this nickel-based alloy. Despite this limitation, calibrated material models provide sufficient accuracy for engineering simulations and structural design applications under moderate strain rates and elevated temperatures.*

Keywords: Aluminium alloy, Equivalent plastic strain, Evolutionary algorithm, Flow stress, Uniaxial stress state

1. Introduction

Structural materials generally exhibit different mechanical behaviour depending on the type and conditions of loading. Understanding this behaviour is essential for accurate material modelling and reliable numerical simulations of structures.

Three materials were selected for the current study. The first material is the corrosion resistant stainless steel AISI 316L, which is commonly applied in the energy and chemical industries due to its high corrosion resistance and good mechanical performance. The second investigated material is the nickel-based superalloy Inconel 718. This alloy retains its mechanical properties at elevated temperatures, making it suitable for demanding applications, particularly in the aerospace sector, where it is used for jet engine components, turbine blades and fastening elements. The third material is the aluminium alloy EN AW 2024-T351, which is characterized by high strength and excellent fatigue resistance. Owing to its favourable strength-to-weight ratio, it is widely used in the automotive and aerospace industries.

The main objective of constitutive modelling of these materials is to cover a wide range of temperatures and strain rates. The results will enable numerical simulations that incorporate a wide spectrum of loading rates and thermal conditions, including the material response under static loading that was achieved by interrupting the tests according to Huang and Young (2014).

2. Material and methods

2.1. Quasi-static, dynamic and high-temperature tensile testing

Experimental data were obtained using a uniaxial tensile test. Test was performed using standardized tensile specimens with circular cross-sections of 6 and 8 mm in diameter having gauge lengths of 30 and 40 mm.

¹ Ing. Radek Novotný: Brno University of Technology, Faculty of Mechanical Engineering, Institute of Solid Mechanics, Mechatronics and Biomechanics; Technická 2896/2; 616 69, Brno; CZ, Radek.Novotny3@vutbr.cz

² doc. Ing. František Šebek, Ph.D.: Brno University of Technology, Faculty of Mechanical Engineering, Institute of Solid Mechanics, Mechatronics and Biomechanics; Technická 2896/2; 616 69, Brno; CZ, sebek@fme.vutbr.cz

Dynamic tensile tests were performed to capture the effect of loading speed, while elevated temperature tests were performed to capture the temperature dependence, all summarized in the Tab. 1 including quasi-static tests (Novotný, 2025).

Tab. 1: Parameters of the uniaxial tensile tests (Novotný, 2025).

Tensile test	Material	Temperature [°C]	Loading rate [mm/min]
Quasi-static	AISI 316L	22	1
	Inconel 718		
	EN AW 2024-T351		
Dynamic	AISI 316L	22	100
	Inconel 718		100
	EN AW 2024-T351		100
	EN AW 2024-T351		200
High-temperature	AISI 316L	400	1
	EN AW 2024-T351	150	
	EN AW 2024-T351	200	

2.2. Static tensile testing

Furthermore, static tensile tests were carried out after Huang and Young (2014). These experiments followed a similar protocol to quasi-static tests, however, included the pauses during loading. Three pauses of 100 seconds each were chosen. These pauses resulted in a decrease in the measured force. A static curve can then be determined from these static drops. It should represent the static behaviour of the material without the influence of quasi-static loading (Novotný, 2025).

3. Constitutive modelling

The Johnson–Cook model was considered as (Johnson and Cook, 1983)

$$\bar{\sigma} = (A + B\bar{\varepsilon}_p^n) \left(1 + C \ln \frac{\dot{\bar{\varepsilon}}_p}{\dot{\bar{\varepsilon}}_0} \right) \left(1 - \left(\frac{T - T_r}{T_m - T_r} \right)^m \right), \quad (1)$$

where $\bar{\sigma}$ is the equivalent stress, A , B and C are the material parameters, $\bar{\varepsilon}_p$ is the equivalent plastic strain, n is the strain hardening exponent, $\dot{\bar{\varepsilon}}_p$ is the equivalent plastic strain rate, $\dot{\bar{\varepsilon}}_0$ is the reference plastic strain rate, T is the temperature, T_r is the reference temperature, T_m is the melting temperature and m is the thermal softening exponent.

All of the material parameters mentioned above were calibrated in MATLAB 2024b using particle swarm optimization (PSO). PSO is a computational method based on the movement of organisms such as a flock of birds or fish schools that are used to find local extremes. The main parameter for PSO is the number of particle swarms. A total of 10^4 particles were used, each particle representing a potential solution to the optimization problem under investigation. The maximum number of iterations was limited to 10^2 and the optimization ends if the change in the objective function value between iterations falls below 10^{-6} . The final set of material parameters is given in the Tab. 2 (Novotný, 2025).

Tab. 2: Material parameters of the Johnson–Cook model (Novotný, 2025).

Material	A [MPa]	B [MPa]	n [-]	C [-]	$\dot{\bar{\varepsilon}}_0$ [s ⁻¹]	T_r [°C]	T_m [°C]	m [-]
AISI 316L	270.0	1130	0.688	0.014	$6 \cdot 10^{-6}$	22	1400	1.244
Inconel 718	380.0	1821	0.718	0.009			1300	–
EN AW 2024-T351	270.0	747.0	0.607	0.009			500	2.250

ANSYS Workbench 2024 R2 and the implicit solver in LS-DYNA were used for numerical simulations. All analyses were calculated as axisymmetric. The specimen geometry was modelled without clamping parts with only half of the gauge length, making the geometry a rectangle with radius and gauge length of the specimens. Shell elements were used to create a structured mesh. The global size of the finite element was 0.1 mm (Novotný, 2025).

A complete Johnson–Cook material model marked *MAT_015 was chosen as the only model defined for the implicit solver in LS-DYNA, which can be used in thermal analysis. This material model has to be supplemented with an equation of state (EOS). The EOS is responsible for calculating the pressure based on changes in volume, density and possibly energy or temperature (Novotný, 2025).

4. Results and discussion

The stress–strain curves obtained from the numerical simulations were compared with the experiments in Figs. 1–3, where the dashed and solid lines refer to the numerical simulations and experiments, respectively. The results indicate that the material model captures the dependence on strain rate and temperature (Novotný, 2025).

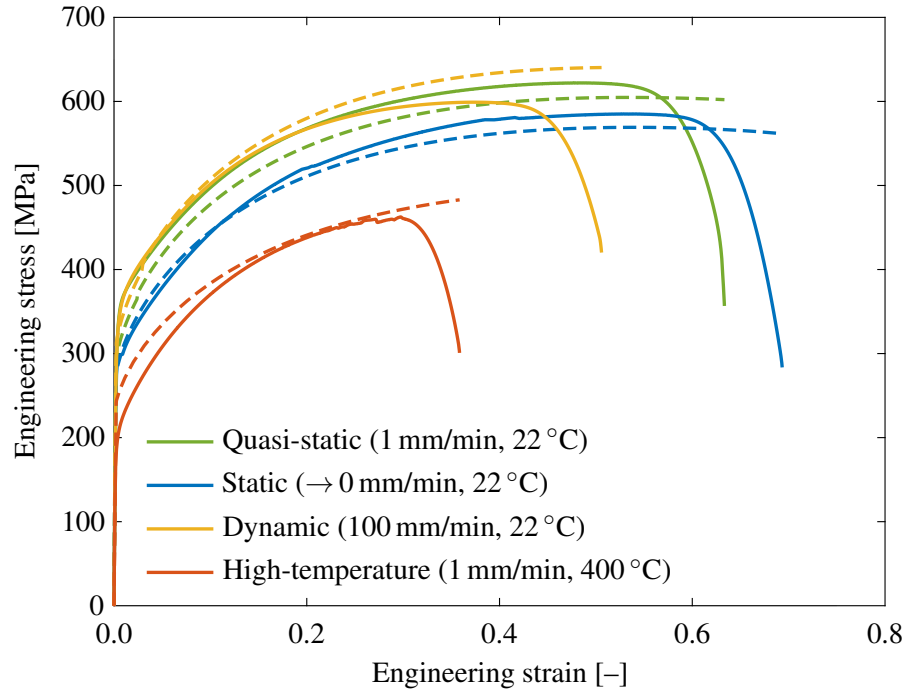


Fig. 1: Stress–stress curves compared from numerical simulations and experiments of AISI 316L.

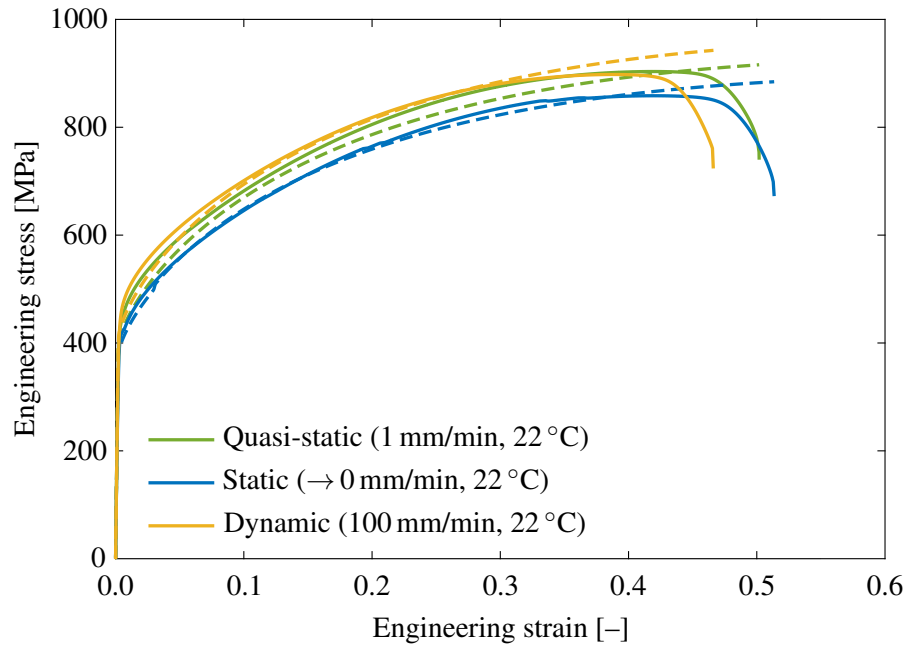


Fig. 2: Stress–stress curves compared from numerical simulations and experiments of Inconel 718.

The largest differences were observed beyond the ultimate tensile strength during necking. This inaccuracy is caused by a slight overestimation of the strain hardening exponent, which, on the other hand, well described the region prior to plastic instability (Novotný, 2025).

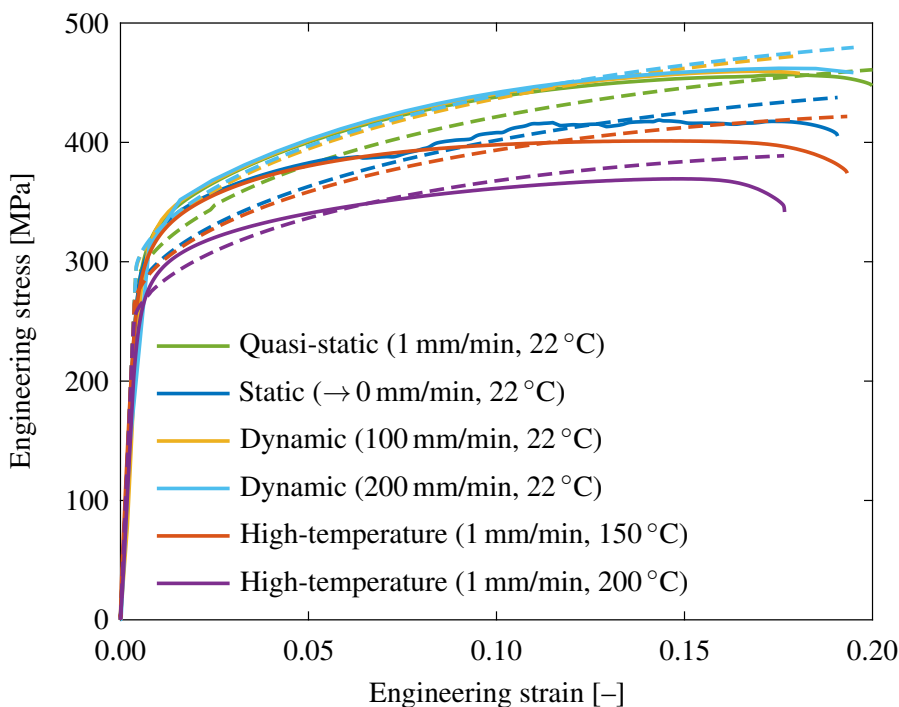


Fig. 3: Stress–stress curves compared from numerical simulations and experiments of EN AW 2024-T351.

5. Conclusions

The present work deals with constitutive modelling, which includes the effects of strain rate and temperature for three metals, AISI 316L, Inconel 718 and EN AW 2024-T351. The percent error was up to 10 % for nine of the numerical simulations, while the remaining two were up to 20 %. It should be noted that the temperature effect was not considered for Inconel 718 due to the absence of thermal testing. The material models presented provide a basis for engineering applications and structural designs, particularly for strain rates up to approximately 0.05 and 0.1 s^{-1} and temperatures up to 400 °C for AISI 316L and 200 °C for EN AW 2024-T351. Future work could focus on extending the proposed methodology to additional material classes. Furthermore, performing a larger number of tests at higher strain rates would enable improved modelling of dynamic events such as impacts and crashes. Additional high-temperature experiments would refine the description of thermal effects and allow identification of the thermal softening exponent for Inconel 718.

Acknowledgments

This work is an output of the project Computational modelling of ductile fracture of identical wrought and printed metallic materials under ultra-low-cycle fatigue created with financial support from the Czech Science Foundation under the registration no. 23-04724S.

References

- Huang, Y. and Young, B. (2014) The art of coupon tests. *Journal of Constructional Steel Research*, 96, pp. 159–175.
- Johnson, G. R. and Cook, W. H. (1983) A constitutive model and data for metals subjected to large strains, high strain rates and high temperatures. In *Proceedings of the 7th International Symposium on Ballistics*, The Hague. International Ballistics Committee, pp. 541–547.
- Novotný, R. (2025) *Analysis of the effect of size, temperature and strain rate on the hardening of metallic materials*. Master’s Thesis, Brno University of Technology.